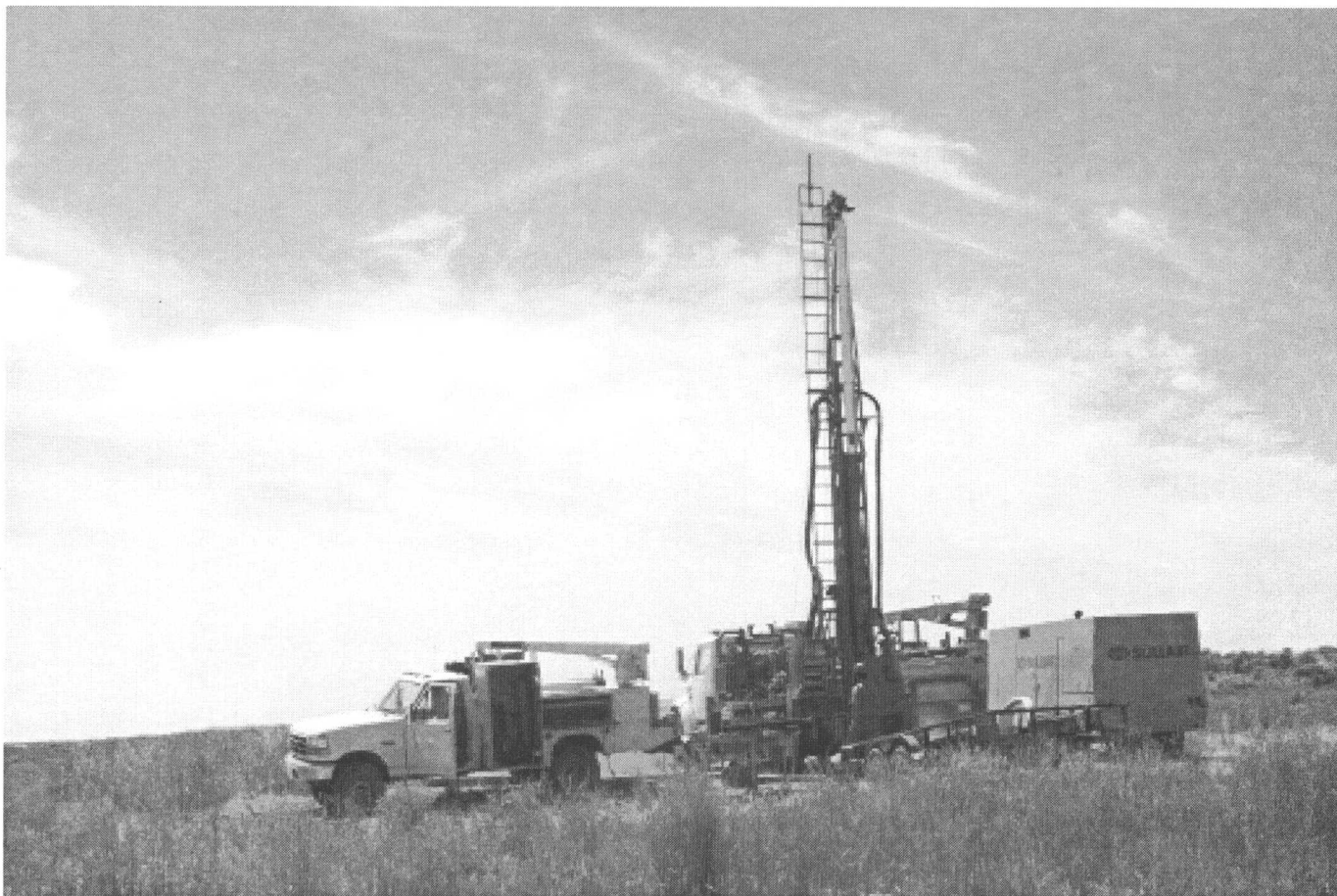


Rec'd
6/29/01

MEASUREMENT OF HYDRAULIC PROPERTIES OF THE B-C INTERBED AND THEIR INFLUENCE ON CONTAMINANT TRANSPORT IN THE UNSATURATED ZONE AT THE IDAHO NATIONAL ENGINEERING AND ENVIRONMENTAL LABORATORY, IDAHO

U.S. GEOLOGICAL SURVEY
WATER-RESOURCES INVESTIGATIONS REPORT 00-4073



Prepared in cooperation with the
U.S. DEPARTMENT OF ENERGY



**MEASUREMENT OF HYDRAULIC PROPERTIES OF
THE B-C INTERBED AND THEIR INFLUENCE ON
CONTAMINANT TRANSPORT IN THE UNSATURATED
ZONE AT THE IDAHO NATIONAL ENGINEERING AND
ENVIRONMENTAL LABORATORY, IDAHO**

By Kim S. Perkins and John R. Nimmo

**U.S. GEOLOGICAL SURVEY
Water-Resources Investigations Report 00-4073**

**Prepared in cooperation with the
U.S. DEPARTMENT OF ENERGY**

**Idaho Falls, Idaho
April 2000**

U.S. DEPARTMENT OF THE INTERIOR
GALE A. NORTON, Secretary

U.S. GEOLOGICAL SURVEY
CHARLES G. GROAT, Director

Any use of trade, product, or firm names in this publication is for descriptive purposes only and does not constitute endorsement by the U.S. Government.

For additional information write to:

U.S. Geological Survey
INEEL, MS 1160
P.O. Box 2230
Idaho Falls, ID 83403

Copies of this report can be purchased from:

U.S. Geological Survey
Information Services
Box 25286, Federal Center
Denver, CO 80225

CONTENTS

Abstract	1
Introduction.....	1
Purpose and scope	3
Previous interbed observations and characterization.....	3
Geohydrologic setting.....	6
Methods	6
Results and discussion	8
Conclusions.....	18
References.....	18

FIGURES

Figure 1. Map showing location of the Idaho National Engineering and Environmental Laboratory and Radioactive Waste Management Complex	2
2. Map showing location of UZ98-2, Radioactive Waste Management Complex, Big Lost River and spreading areas	4
3. Cross section showing subsurface geology at the Radioactive Waste Management Complex and vicinity.....	5
4. Graph showing field matric potential and moisture content profiles	17

TABLES

Table 1. Summary of interbed core properties	9
2. Conductivity and moisture retention data	10
3. Fitted parameters	14
4. Condensed texture data	15

CONVERSION FACTORS, VERTICAL DATUM, AND ABBREVIATED UNITS

	Multiply	By	To obtain
Centimeter per second (cm/s)		0.3937	Inch per second
Meter (m)		3.281	Foot
Square kilometer (km ²)		0.3861	Square mile
Cubic centimeter (cm ³)		0.06102	Cubic inch
Gram per cubic centimeter (g/cm ³)		62.4220	Pound per cubic foot

For temperature, degrees Celsius (°C) can be converted to degrees Fahrenheit (°F) by using the equation:
 $^{\circ}\text{F} = (1.8)(^{\circ}\text{C}) + 32.$

Measurement of Hydraulic Properties of the B-C Interbed and their Influence on Contaminant Transport in the Unsaturated Zone at the Idaho National Engineering and Environmental Laboratory, Idaho

by Kim S. Perkins and John R. Nimmo

Abstract

The intensely layered character of the 200-m thick unsaturated zone near the Radioactive Waste Management Complex (RWMC) Subsurface Disposal Area (SDA) at the Idaho National Engineering and Environmental Laboratory (INEEL) critically affects both vertical and horizontal water fluxes. Because of the potential for radionuclide migration from the SDA to the Snake River Plain aquifer, it is important to investigate the role of the unsaturated zone in contaminant transport processes. The unsaturated zone consists of thick layers of fractured basalts interbedded with thinner layers of sediment. These interbeds and basalts were deposited approximately 50,000 to 450,000 years ago during the late Pleistocene. As a part of a drilling program to develop a standard methodology for subsurface characterization and risk assessment at INEEL, hydraulic properties of the 34-m deep sedimentary interbed (known as the B-C interbed (Anderson and Lewis, 1989)) have been measured at one location in the vicinity of the SDA, including particle size distributions, water retention functions, saturated and unsaturated hydraulic conductivity, and related properties. In porous media, water flux is usually modeled in terms of Darcy's law for steady flow and Richards' equation for transient flow. Both of these formulations require knowledge of the unsaturated hydraulic conductivity (K) of the media, a property that is difficult to measure and highly sensitive to variations in water content. The transient case additionally requires knowledge of the water retention relation, which similarly varies to a high degree within the medium. The interbeds may play several critical roles in long-range transport processes: (a) retardation of downward-moving water as it encounters layer boundaries, (b) gener-

ation of perched water, (c) homogenization of preferential flow that has been focused by basalt fractures, and (d) the formation of long-range, highly conductive horizontal flow paths for contaminants. Within these sedimentary layers, there may be little or no impediment to lateral flow. Drastic differences in hydraulic properties between the basalt and interbeds, and within the interbeds themselves, are likely to promote such flow.

INTRODUCTION

The Radioactive Waste Management Complex (RWMC) occupies about 0.75 km² of the Idaho National Engineering and Environmental Laboratory (INEEL) in southeastern Idaho (fig. 1). From 1952 to 1970, chemical, low-level radioactive, and transuranic wastes were buried in trenches and pits excavated into the surficial sediments of the Subsurface Disposal Area (SDA) of the RWMC. Since 1970, transuranic waste has been stored on above-ground asphalt pads in retrievable containers. Low-level radioactive and mixed chemical wastes were buried through 1983. Since that time, only low-level radioactive waste has been buried in the SDA (Maheras and others, 1994). Radionuclides have been detected in core and drill cuttings from several boreholes drilled into the surficial sediments and underlying rock units at the RWMC (Barraclough and others, 1976; Laney and others, 1988).

The unsaturated zone at the RWMC consists of thick layers of fractured basalts interbedded with thinner, unconsolidated layers of sediment. Perched water has been detected in and above these sedimentary interbeds at the RWMC. This perched water, attributed either to flooding from localized runoff or to lateral unsaturated-zone flow

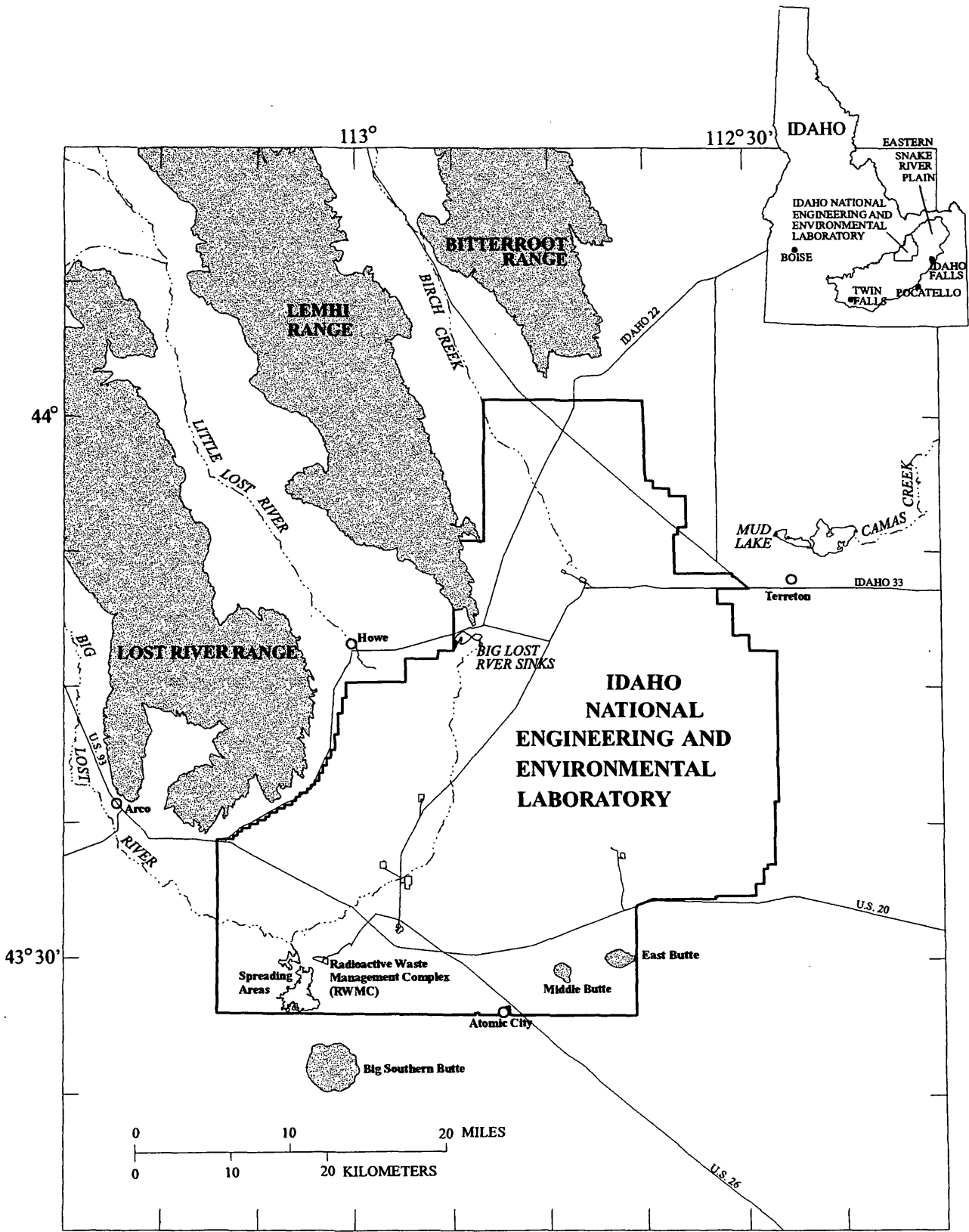


Figure 1. Location of the Idaho National Engineering and Environmental Laboratory and Radioactive Waste Management Complex.

from nearby flood-control structures associated with the Big Lost River, may influence the transport of contaminants in the unsaturated zone beneath the RWMC. The occurrence of perched water is controlled by the hydraulic properties of the interbeds. However, little is known about the distribution and character of those properties and their role in contaminant transport.

Purpose and Scope

Two geotechnical coreholes, UZ98-1 and UZ98-2, were drilled in 1998 through the B-C interbed at a site approximately 1.2 km southwest of the RWMC and adjacent to spreading area B, one of the flood-control structures (fig. 2). The purpose of these coreholes was to obtain cores of unconsolidated sediments to evaluate laboratory hydraulic properties of these sediments. This report describes the hydraulic characteristics of the minimally disturbed core samples recovered in September, 1998 from the B-C interbed in corehole UZ98-2. These samples were carefully re-cored in the laboratory into the appropriate retainers for measurement of hydraulic conductivity using the steady-state centrifuge (SSC) method (Nimmo and Mello, 1991; Conca and Wright, 1998). Hydraulic conductivity (K) and matric potential (ψ) measurements were carried out on 18 samples from various depths in the B-C interbed. Trimmings from the re-coring process along with bulk samples recovered in drilling were used in measuring 40 particle-size distributions along the 10.4 m profile. This study was conducted in cooperation with the U.S. Department of Energy.

Previous Interbed Observations and Characterization

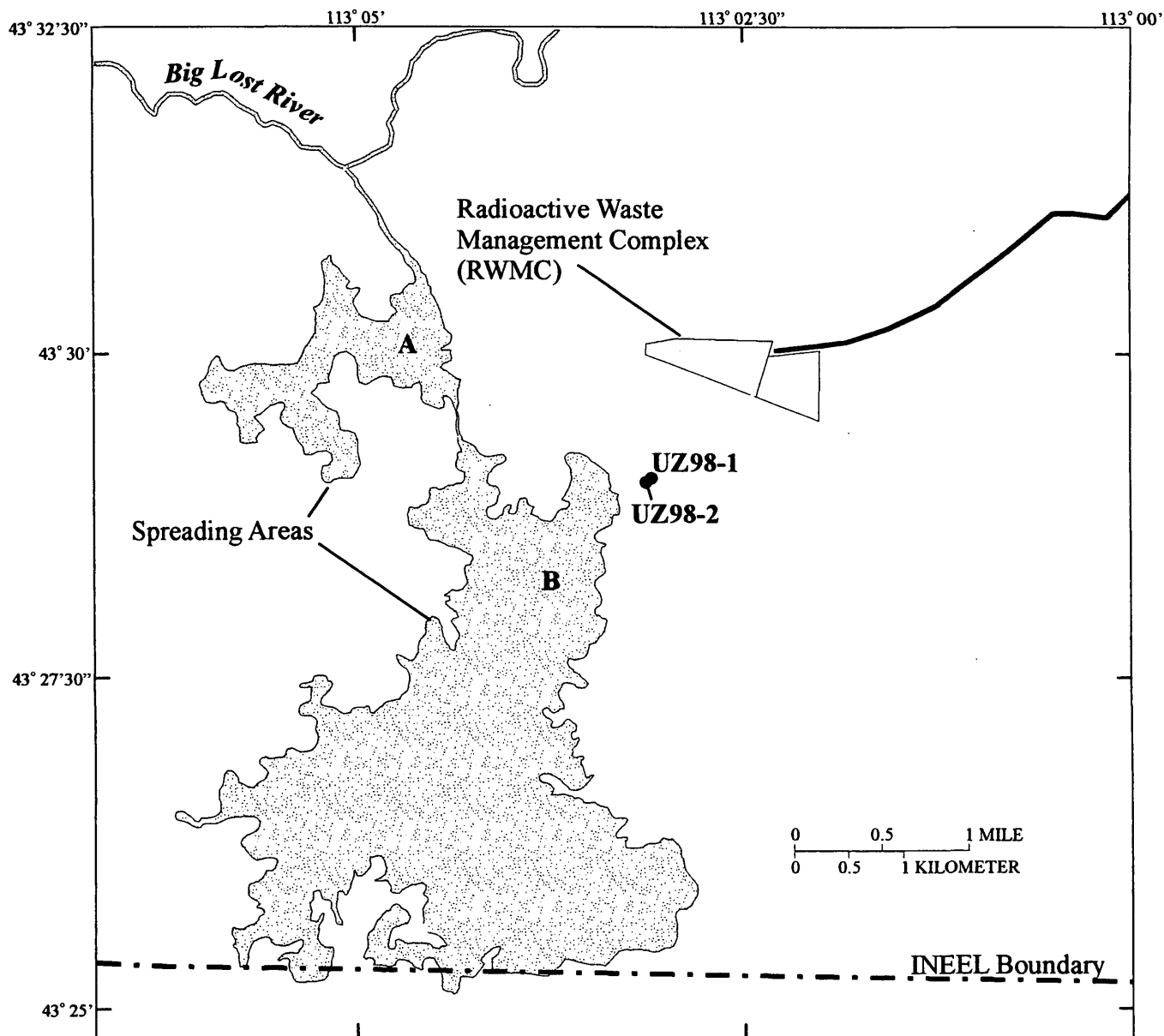
Perched water, detected in association with the B-C and deeper interbeds beneath the RWMC and surrounding area (fig. 3) occurs both seasonally and permanently, and may be due, in part, to lateral flow from spreading area infiltration (Rightmire and Lewis, 1987; Hubbell, 1990). Hubbell (1990) presented water-level records from two SDA boreholes as evidence suggesting that perched water-level recovery rates are correlated with the historic record of inflows into the spreading areas. Anderson and Lewis (1989) suggested

that sedimentary layers may control vertical flow depending on grain size and sorting characteristics. They noted that lateral flow and perching of water may take place along some clay and silt layers, and that discontinuous layers may divert flow toward underlying or adjacent basalt flows. Sedimentary interbeds beneath the RWMC are characterized by abrupt lateral changes in thickness related to the topography of underlying basalt flows (Anderson and Lewis, 1989). Anderson and Lewis (1989) describe one structure on the top of basalt-flow group C in the western part of the SDA, where the thickness of the B-C interbed changes abruptly from 0 m on a basalt ridge to more than 6 m in an adjacent depression. Infiltrating water may migrate towards such depressions at some sediment-basalt interfaces, resulting in areas of localized perched water or preferential flow.

Burgess (1995) noted that, during a 1994 large-scale infiltration experiment, perched water associated with the B-C interbed was observed within and outside of the infiltration basin. Data obtained during this test show that the B-C interbed may act as a semi-permeable barrier to vertical flow and that interbed topography is the predominant control on lateral movement of perched water.

Rightmire and Lewis (1987) used isotopic analysis of $\delta^{18}\text{O}$ (oxygen) and $\delta^2\text{H}$ (deuterium) to show that perched water might be derived, in part, from lateral flow of spreading area water in the unsaturated zone. They found that the isotopic content in perched water samples from beneath the RWMC could be attributed to a water source at a higher altitude than the surface of the Snake River Plain, meaning that the water may have come from the spreading areas. They hypothesized that water accumulates as a perched mound and then moves laterally to the RWMC, 1.5 km to the northeast.

Anderson and Lewis (1989) used sediment cores and geophysical logs to determine the areal extent and thickness of basalt flows and sedimentary interbeds. They estimated an average interbed thickness of 1.5 m for the A-B, 4.0 m for the B-C, and 5.2 m for the C-D. It has also been estimated that the B-C interbed slopes approximately 3.8 m/km from west to east (Anderson and Lewis, 1989; Barraclough and others, 1976).



EXPLANATION
UZ98-2 ● GEOTECHNICAL COREHOLE -- Entry, UZ98-2, is the local well identifier

Figure 2. Location of UZ98-2, Radioactive Waste Management Complex, Big Lost River, and spreading areas.

EXPLANATION

- B **BASALT** — Basalt-flow group composed of one or more related flows. Letter, B, indicates sequence of group from top to bottom of section. Locally includes cinders and thin layers of sediment
- CLAY, SILT, SAND, AND GRAVEL** — Major sedimentary interbed between volcanic flow groups. Locally includes cinders and basalt rubble
- GEOLOGIC CONTACT** — Queried where uncertain
- WELL** — Entry, 88, is local well identifier. Arrow indicates water level in aquifer in June, 1988

Location of Section

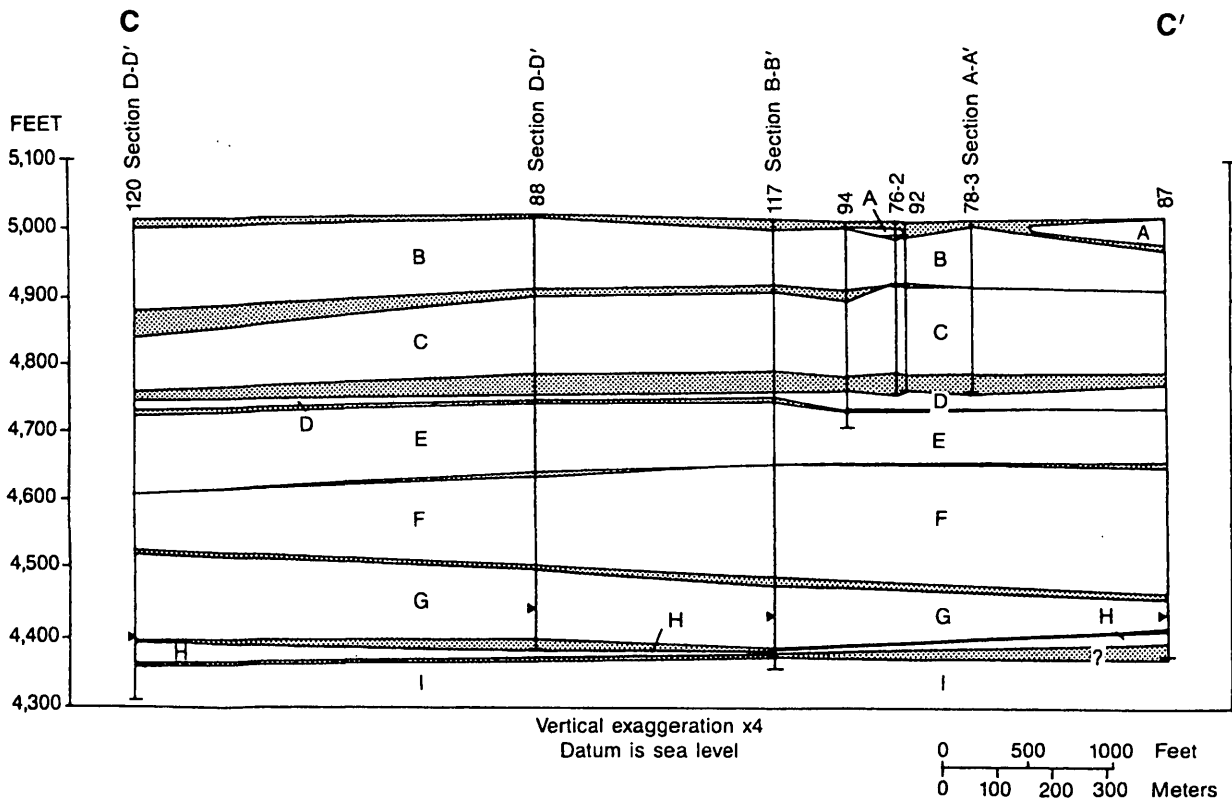
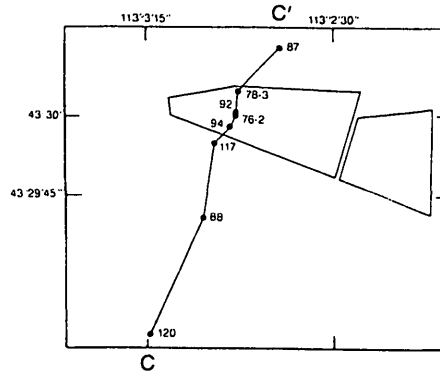


Figure 3. Subsurface geology at the Radioactive Waste Management Complex and vicinity (from Anderson and Lewis, 1989, p. 29)

McElroy and Hubbell (1990) present results of hydraulic property measurements from interbeds beneath the RWMC. They selected a total of 35 subcores from various locations and depths for hydraulic property analysis, including 1 sample from the B-C interbed. The results indicate a range in saturated hydraulic conductivity for all samples from 1×10^{-8} to 7×10^{-3} cm/s, the B-C interbed sample having the lowest value. Within the C-D interbed, they noted decreasing permeability with depth in three of five boreholes, while the other two showed low-permeability clays at the top of the interbed. Burgess (1995) observed similar low-permeability clay layers at the top of the B-C interbed during well and corehole installation associated with the large-scale infiltration test of 1994.

Hughes (1993) used cores from 9 wells and gamma logs from 24 wells within and around the RWMC to describe the sedimentary interbeds. According to this investigation, the B-C interbed ranges from 0.6 to 9.8 m thick where present. The absence of the B-C interbed in four of the wells used in the analysis was associated with topographic highs in the underlying basalt. Hughes (1993) also noted that lateral variations in grain size and thickness are very evident in this interbed, and that the material is generally coarse, ranging from silty sand to gravel.

Geohydrologic Setting

The eastern Snake River Plain is a structural basin about 325 km long and 80 to 110 km wide, bounded by mountain ranges and high plateaus. Streams within alluvial valleys separating the mountain ranges to the north and northwest flow onto the plain and the INEEL in response to rainfall and snowmelt. The eastern Snake River Plain is underlain by a sequence of basaltic lava flows interbedded with sedimentary deposits. The sediments consist of fluvial, lacustrine, and eolian deposits of clay, silt, sand, and gravel. Rhyolitic lava flows and tuffs crop out locally at the surface and occur at depth below the basalt-sediment sequence (Mann, 1986). The INEEL occupies about 2,300 km² of semi-arid, sagebrush-covered terrain on the northwestern side of the plain. The RWMC is in the southwestern part of the INEEL

in a shallow topographic depression. The surficial sediments at the RWMC consist of about 0.6 to 7.0 m of clay, silt, sand, and gravel. Substantial sedimentary interbeds occur at depths of approximately 9 m (known as the A-B interbed), 34 m (known as the B-C interbed), and 73 m (known as the C-D interbed) below land surface (Fig. 3). Because the C-D interbed has been detected in all wells drilled within the SDA it has been considered the most continuous barrier to vertical flow beneath the SDA, though recent drilling has shown that the interbed may be absent to the east and northeast of the SDA (Magnuson, 2000, written communication). The A-B and B-C interbeds are discontinuous, although the B-C underlies a large part of the RWMC (Anderson and Lewis, 1989). Other sedimentary deposits of lesser areal extent occur at various depths. Boreholes and wells at the RWMC penetrate about 215 m of basaltic lava flows and sedimentary deposits. Most boreholes are completed in the upper 90 m of the unsaturated zone; thus, the extent of the A-B, B-C, and C-D deposits is better known than that of the deeper interbeds. The stratigraphic sequence at the unsaturated zone test site is similar to the stratigraphic sequence beneath the RWMC.

Methods

During the drilling of borehole UZ98-2, B-C interbed sediment was cored into polycarbonate liners (roughly 8.6 cm inner diameter) and capped off at the ends. Within a few hours of sampling, these cores were taken to a nearby lab and weighed for later estimation of field water content. Small holes (0.95 cm) were carefully drilled through the liners of four sections of core to allow the temporary insertion of a tensiometer. A hole (slightly < 0.95 cm) was cored into the sediment using a handmade stainless steel coring device to allow the tensiometer to be inserted into the center of the core. The tensiometer consisted of a 0.953 cm, 1-bar high-flow ceramic cup (Soilmoisture Equipment Corp., Goleta, CA)¹ epoxied to a brass tube connected to a solid state pressure transducer. The transducer was calibrated and matrix

1. The use of brand names does not constitute endorsement by the USGS.

potential values calculated to correspond to field water contents.

Samples were then transported to the USGS Menlo Park Unsaturated Zone Flow Laboratory for further analysis. The intact cores were weighed prior to recoring to estimate any weight loss since the time of drilling. Samples were then cut into sections approximately 10.2 cm long using a dental-type tool with a circular blade. Each section, unless there was obvious disturbance, was then recored using a mechanical recoring device. Liners were secured by clamps as the material was slowly extruded upward into a 5.2 cm long, 3.3 cm diameter retainer with a sharp-edged custom-made stainless-steel coring attachment. The retainers used are designed specifically to fit into the buckets of the UFA¹ centrifugal rotor, which was used in the unsaturated hydraulic conductivity measurements (Conca and Wright, 1998). This process was done as rapidly as possible to minimize any further water loss due to evaporation. Once in the retainers, the samples were weighed again to later calculate estimates of field water content.

Trimblings from the recoring process and bulk samples were used to determine particle size distributions and color for each section. A Coulter LS-230 Particle Size Analyzer¹ was used to characterize particle size distributions by optical diffraction. The range of measurement is 0.04-2000 microns which is composed of 116 separate size bins. Any particles above 2000 microns were sieved out and later integrated into the size-distribution results. The fraction below 2000 microns was carefully disaggregated using a mortar and rubber-tipped pestle, then split with a riffle splitter to obtain appropriate random samples for analysis. The material was sonicated for 60 seconds prior to each run.

The standard falling head method for obtaining saturated hydraulic conductivity (K_{sat}) was modified to be performed in a centrifuge by Nimmo and Mello (1991). This method, with calculations adapted specifically for the UFA centrifuge, was performed at a speed of 300 rpm. Saturated hydraulic conductivity was calculated with the following modified equation

$$K = [(-2la)/(A\rho\Delta t g)] \ln \left(\frac{gz_f + \omega^2 r_b^2}{gz_i + \omega^2 r_b^2} \right)$$

where l is sample length, a is the cross sectional area of the inflow reservoir, A is the cross sectional area of the sample, ρ is the density of the fluid (water in this case), t is time, g is gravitational force, z is the height of water in the reservoir (initial and final), r is the radius of rotation at the sample bottom, and ω is angular speed in radians per second. This technique allows for rapid measurement on samples that are fine textured with very low K_{sat} values. The lab-saturated moisture content was determined by weight at the end of the saturated conductivity measurement.

The steady state centrifuge (SSC) method used for obtaining unsaturated hydraulic conductivity is the "UFA" version (Conca and Wright, 1998) of the method originally developed by Nimmo and others (1987). Steady-state unsaturated flow through a core sample is achieved relatively quickly using centrifugal force to drive the liquid flow, with flux through the sample maintained precisely by a metering pump. A rotating seal assembly conducts the water from the pump to the spinning sample. K can be determined over a range of water contents by choosing appropriate flow rates and centrifuge speeds. The procedure starts with a K_{sat} measurement, which saturates the sample and indicates the maximum flux to apply during a sequence of unsaturated runs. After the start from saturation, each step in the unsaturated sequence produces data for a point on the drying curve with a unique K , θ , and ψ . The steps must proceed through progressively drier conditions and lower K values. The driving force and the flow rate at the wettest run in the sequence must be selected so as not to exceed the flow at saturation. Each run continues until the steadiness of flow can be verified. This occurs when the sample water content and the flux through the sample become constant. The water content is determined by weighing the sample between runs. The flux into the sample has a known value determined by the pump. The flux out of the sample is measured by repeated weighing of the outflow reservoir, or by use of a centrifuge strobe light assembly and viewing port to monitor the volumetrically calibrated outflow reservoir as the rotor is spinning. For the samples in this study, the required time to achieve steady conditions varied from one hour for

high K values, to one or more days for low K values. The oven-dry weight of the soil, determined later, allows the calculation of the water content for each steady-state run. When desired to supplement the water content value associated with K, the matric potential is measured at the end of a steady-state run. This is done with a nonintrusive touch tensiometer for relatively wet conditions, or with the "filter paper" method (Campbell and Gee, 1986) in cases where suctions exceed 800 cm.

The SSC method as described above was used in this analysis with K and θ measured in each run, and ψ measured in most. There was no observable compaction of these samples due to centrifugal force, so the effect of such compaction on the hydraulic properties was taken to be negligible.

Particle-density measurements were performed with the pycnometer method (Blake and Hartge, 1986) on four representative samples chosen from various depths. Porosity was then calculated using the measured bulk and particle density values (Danielson and Sutherland, 1986).

RESULTS AND DISCUSSION

The physical and hydraulic property measurements provided through this study will enhance the understanding of hydrologic processes taking place in the B-C sedimentary interbed. The measured properties include: bulk density, particle density, particle-size distributions, soil-moisture retention, saturated hydraulic conductivity, and hydraulic conductivity as a function of water content.

A summary of the 18 interbed core sample properties is provided in Table 1, including calculated porosity, field moisture content, lab-saturated moisture content, percent field saturation (calculated using lab saturation data), saturated conductivity, and USDA textural classification. The lab-saturated moisture content may be higher than a field-saturated moisture content due to the compression of trapped air under the applied centrifugal force. Particle density was measured on four representative samples from depths of 41.76, 44.81, 48.16, and 49.68 m (Blake and Hartge, 1986). The results were 2.66, 2.64, 2.64, and

2.65 g/cm³, respectively. A value of 2.65 g/cm³ was used in the calculation of porosity.

Unsaturated hydraulic conductivity and moisture retention data for samples from corehole UZ98-2 are presented in tabular form in Table 2. These data were used to determine the commonly used fitted parameters α and n of the van Genuchten equation (1980). The shape factors, α (an empirical parameter whose inverse is often referred to as the air entry value (van Genuchten and others, 1991)) and n, are required input for many of the available numerical simulation codes describing variably saturated flow. These parameter values were determined by optimization using retention data alone, and by simultaneously optimizing to retention and conductivity data with a combination of the van Genuchten (1980) and Mualem (1976) equations using the RETC program (van Genuchten and others, 1991). This program performs a nonlinear least squares fit to the measured data. The results of this analysis are included in Table 3.

The interbed at this location has three distinct sections. The uppermost 0.3 m of the profile at this location is a red (2.5YR 5/6 (Munsell Soil Color)), highly oxidized "baked zone" of gravelly sand which was directly overlain by basalt flows. The underlying 4.6 m of material is dark grayish-brown (10YR 4/2) and sandy in texture with intermittent gravel layers present in the intervals of 40.23-40.54, 42.98-43.09, 43.21-43.31, and 44.81-45.11 m, suggesting a fluvial environment. The lower 5.5 m of the profile is a relatively uniform pale yellow (2.5Y 7/3) silt loam with fine, thin sand lenses throughout, possibly deposited in a low energy fluvial environment. Particle-size distributions are presented in condensed tabular format in Table 4 and graphical format in the Appendix. Silt loam particle-size distribution curves that have a distinct secondary peak in the sand range are likely due to the presence of sand lenses.

Table 1: Summary of interbed core properties

Depth (meter)	Calculated porosity	Field moisture content	Lab saturated moisture content	Percent saturation (lab/field water content)	Saturated hydraulic conductivity (centimeter per second)	Texture (USDA)
42.98-43.09	.5042	.2400	.4381	55.8	3.90E-03	Sand
43.09-43.21	.5131	.2565	.4464	57.5	3.90E-03	Sand
43.21-43.31	.5170	.3576	.4497	79.5	3.90E-03	Sand
43.31-43.43	.4881	.2568	.4230	60.7	3.90E-03	SandyLoam
45.21-45.31	.3842	.3331	.3625	91.8	6.08E-05	Silt Loam
48.16-48.26	.4721	.4201	.4231	99.3	5.66E-07	Silt Loam
48.26-48.36	.4519	.4317	.4326	99.8	3.44E-07	Silt Loam
48.44-48.55	.4541	.3524	.3644	96.4	1.25E-05	Silt Loam
48.92-49.02	.4442	.3645	.3984	91.5	4.76E-07	Silt Loam
49.02-49.12	.4397	.3791	.4130	91.8	1.09E-06	Silt Loam
49.23-49.30	.4517	.3360	.4067	82.6	1.48E-05	Silt Loam
49.30-49.38	.4699	.3113	.4004	77.7	2.78E-05	Silt Loam
49.79-49.89	.4514	.2901	.3473	83.5	3.16E-06	Silt Loam
49.89-49.99	.4598	.3392	.3775	89.9	1.70E-05	Silt Loam
49.99-50.06	.4385	.4082	.4369	93.4	8.18E-06	Silt Loam
50.06-50.10	.4558	.3715	.4268	87.0	1.64E-05	Silt Loam
50.10-50.30	.4474	.4290	.4315	99.4	2.35E-07	Silt Loam
50.30-50.40	.4551	.4135	.4344	95.2	4.75E-07	Silt Loam

Table 2: Conductivity and moisture retention data

Sample depth (meter)	Volumetric water content	Conductivity (centimeter per second)	Matric potential (centimeter water)
42.98-43.09	0.4381	3.90E-03	0.0
	0.2907	1.85E-04	a
	0.2008	4.80E-05	-32.1
	0.143	1.81E-05	-49.2
	0.1239	8.15E-06	-51.4
	0.112	3.33E-06	
	0.1036	1.37E-06	-65.5
	0.0969	4.17E-07	
	0.0872	9.13E-08	-112.6
	0.0776	3.15E-08	
	0.0728	5.81E-09	-132.3
43.09-43.21	0.4464	3.90E-03	0.0
	0.2669	1.85E-04	
	0.1799	4.89E-05	-36.4
	0.1176	1.83E-05	-53.5
	0.0991	7.41E-06	
	0.091	3.33E-06	
	0.0836	1.37E-06	-61.4
	0.078	4.55E-07	-70.8
	0.0681	8.34E-08	-94.4
	0.0618	3.15E-08	
	0.0558	5.34E-09	
43.21-43.31	0.4497	3.90E-03	0.0
	0.1808	1.74E-05	-61.2
	0.154	7.95E-06	-74.1
	0.1326	3.62E-06	-88.4
	0.1281	1.36E-06	-90.8
	0.1192	4.54E-07	-103.0
	0.1108	8.92E-08	-138.7

Table 2: Conductivity and moisture retention data--Continued

Sample depth (meter)	Volumetric water content	Conductivity (centimeter per second)	Matric potential (centimeter water)
	0.1041	3.44E-08	-154.8
	0.0926	5.34E-09	-234.2
43.31-43.43	0.423	3.90E-03	0.0
	0.1486	1.77E-05	-41.1
	0.1302	7.41E-06	-46.9
	0.1124	3.33E-06	-57.1
	0.1075	1.25E-06	-71.1
	0.096	4.17E-07	-83.3
	0.091	8.34E-08	-142.1
45.21-45.31	0.3513	6.08E-05	0.0
	0.3073	3.22E-06	-55.9
	0.2927	1.23E-06	-88.6
	0.2847	4.54E-07	-115.2
	0.2755	8.93E-08	-138.3
	0.2592	3.35E-08	-218.5
	0.2429	5.70E-09	-302.2
48.16-48.26	0.4231	5.66E-07	0.0
	0.406	4.17E-07	-163.7
	0.3815	8.34E-08	-389.8
	0.3588	3.15E-08	-776.5
	0.3451	5.34E-09	
48.26-48.36	0.4326	3.44E-07	0.0
	0.4065	8.34E-08	-418.2
	0.375	3.15E-08	-640.2
	0.3505	5.34E-09	-4324.6
48.44-48.55	0.3644	1.25E-05	0.0
	0.3347	3.24E-06	-70.6
	0.3064	1.35E-06	-218.3
	0.2783	3.98E-07	-324.9

Table 2: Conductivity and moisture retention data--Continued

Sample depth (meter)	Volumetric water content	Conductivity (centimeter per second)	Matric potential (centimeter water)
	0.2527	8.11E-08	-442.2
	0.2327	3.14E-08	-504.7
	0.2145	5.97E-09	-949.0
48.92-49.02	0.3725	4.76E-07	0.0
	0.3608	4.17E-07	-96.7
	0.337	8.34E-08	-2028.0
	0.3188	3.15E-08	
	0.2983	5.34E-09	-3476.0
49.02-49.12	0.3876	1.09E-06	0.0
	0.3435	4.17E-07	
	0.3141	8.34E-08	-1874.0
	0.2891	3.15E-08	
	0.2684	5.34E-09	-2540.0
49.23-49.30	0.4067	1.48E-05	0.0
	0.3177	4.27E-06	-145.3
	0.3083	3.50E-06	-161.2
	0.2836	1.28E-06	-214.9
	0.2608	4.08E-07	-284.5
	0.2396	8.31E-08	-385.2
	0.2198	3.20E-08	-531.2
	0.1972	5.53E-09	-1320.8
49.30-49.38	0.4004	2.78E-05	0.0
	0.3303	4.34E-06	-107.2
	0.3251	3.53E-06	-119.0
	0.3051	1.30E-06	-162.0
	0.2875	4.28E-07	-189.0
	0.2731	8.26E-08	-400.0
	0.2522	3.19E-08	-559.0
	0.2318	5.32E-09	-869.2

Table 2: Conductivity and moisture retention data--Continued

Sample depth (meter)	Volumetric water content	Conductivity (centimeter per second)	Matric potential (centimeter water)
49.79-49.89	0.3473	3.16E-06	0.0
	0.2842	3.06E-06	-83.7
	0.2624	1.28E-06	-109.4
	0.2388	4.35E-07	-167.6
	0.2133	8.26E-08	-228.8
	0.1927	3.20E-08	-253.4
	0.1682	5.41E-09	-1550.1
49.89-49.99	0.3775	1.70E-05	0.0
	0.274	3.54E-06	-113.4
	0.2666	1.32E-06	-121.8
	0.2518	4.48E-07	-168.2
	0.2421	8.51E-08	-200.6
	0.2266	3.37E-08	-262.0
	0.2145	5.18E-09	-608.8
49.99-50.06	0.4369	8.18E-06	0.0
	0.3792	1.27E-06	-184.5
	0.3621	4.02E-07	-259.4
	0.3516	8.26E-08	-421.8
	0.3174	3.16E-08	-632.9
	0.2977	5.53E-09	-1074.4
	50.06-50.10	0.4268	1.64E-05
0.3399		1.20E-06	-254.1
0.3152		4.11E-07	-373.7
0.286		8.42E-08	-497.0
0.2623		3.23E-08	-933.3
0.2393		6.78E-09	-1335.1
50.10-50.30		0.4315	2.35E-07
	0.4228	2.34E-07	-69.3
	0.4078	5.31E-08	-580.9

Table 2: Conductivity and moisture retention data--Continued

Sample depth (meter)	Volumetric water content	Conductivity (centimeter per second)	Matric potential (centimeter water)
	0.4011	2.70E-08	-735.7
	0.3979	5.42E-09	-1200.0
50.30-50.40	0.4344	4.75E-07	0.0
	0.4337	2.36E-07	-60.1
	0.4077	5.65E-08	-562.3
	0.4031	4.28E-08	-608.3
	0.3948	5.85E-09	-1268.0

a. Where blanks exist in table, measurements were not done.

Table 3: Fitted parameters

Depth (meter)	van Genuchten-Mualem α (centimeter ⁻¹)	van Genuchten α	van Genuchten- Mualem n	van Genuchten n
42.98-43.09	.0671	.0822	1.907	1.783
43.09-43.21	.0521	.0507	2.297	2.309
43.21-43.31	.0585	.0946	1.691	1.546
43.31-43.43	.0739	.3136	1.823	1.430
45.21-45.31	.0087	.0331	1.435	1.166
48.16-48.26	.0003	.0163	1.203	1.044
48.26-48.36	.0004	.0042	1.273	1.075
48.44-48.55	.0043	.0059	1.408	1.312
48.92-49.02	.0005	.0004	1.749	2.260
49.02-49.12	.0007	.0061	1.851	1.421
49.23-49.30	.0056	.0157	1.509	1.261
49.30-49.38	.0069	.0232	1.358	1.178
49.79-49.89	.0072	.0351	1.493	1.205
49.89-49.99	.0101	.0737	1.437	1.157
49.99-50.06	.0033	.0079	1.316	1.175
50.06-50.10	.0038	.0055	1.382	1.284
50.10-50.30	.0005	.0148	1.352	1.028
50.30-50.40	.0006	.0041	1.276	1.056

Table 4: Condensed texture data (USDA classification)

Sample depth (meter)	Percent clay less than 2 microns	Percent silt 2-50 microns	Percent very fine sand 50-100 microns	Percent fine sand 100-250 microns	Percent medium sand 250-500 microns	Percent course sand 500-1000 microns	Percent very coarse sand 1000- 2000 microns	Percent gravel less than 2000 microns
40.23-40.54	1	6	7	21	25	17	7	16
41.76-42.06	4	40	26	15	7	6	2	0
42.98-43.09	0	3	2	14	46	26	3	7
43.09-43.21	0	2	3	19	52	23	1	0
43.21-43.31	0	5	7	31	39	12	2	3
43.31-43.43	0	4	4	23	51	18	0	0
43.42 (transi- tion)	2	22	29	46	0	0	0	0
44.81-45.11	0	3	1	5	16	33	15	27
45.21-45.31	4	28	10	25	12	12	7	4
45.11-45.42	10	62	13	6	4	5	0	0
46.33-46.48	13	61	11	15	0	0	0	0
48.16-48.26	15	74	11	1	0	0	0	0
48.26-48.36	14	71	9	6	0	0	0	0
48.36-48.55	12	66	12	10	0	0		0
48.44-48.55	8	56	10	16	0	0	0	0
48.55-48.67	10	67	20	3	0	0	0	0
48.67-48.76	9	65	18	8	0	0	0	0
48.76-48.84	16	78	3	3	0	0	0	0
48.84-48.90	16	71	5	8	0	0	0	0
48.92 (transi- tion)	7	46	18	29	0	0	0	0
48.92-49.02	14	82	4	0	0	0	0	0
49.02-49.12	12	75	13	0	0	0	0	0
49.12	9	49	14	12	13	3	0	0
48.92-49.07	15	80	5	0	0	0	0	0
49.23-49.30	10	58	15	16	1	0	0	0

Table 4: Condensed texture data (USDA classification)--Continued

Sample depth (meter)	Percent clay less than 2 microns	Percent silt 2-50 microns	Percent very fine sand 50-100 microns	Percent fine sand 100-250 microns	Percent medium sand 250-500 microns	Percent course sand 500-1000 microns	Percent very coarse sand 1000- 2000 microns	Percent gravel less than 2000 microns
49.30-49.38	10	62	13	14	1	0	0	0
49.38-49.45	13	76	11	0	0	0	0	0
49.45-49.56	14	84	2	0	0	0	0	0
49.56-49.7	12	81	7	0	0	0	0	0
49.68	17	81	2	0	0	0	0	0
49.68-49.78	15	69	10	6	0	0	0	0
49.78-49.89	10	76	13	1	0	0	0	0
49.89-49.99	13	52	9	24	2	0	0	0
49.99-50.06	15	75	9	1	0	0	0	0
50.06-50.10	13	73	10	4	0	0	0	0
50.10-50.30	16	84	0	0	0	0	0	0
50.30-50.40	18	81	1	0	0	0	0	0
50.40-50.50	23	77	0	0	0	0	0	0
50.50-50.60	21	71	7	1	0	0	0	0
50.60	22	77	1	0	0	0	0	0

As is relatively common in drilling within and around the RWMC (Barraclough and others, 1976; Rightmire and Lewis, 1987), standing water was observed in the UZ98-2 borehole within a few days of completion. The results from the determination of field-moisture content show that some of the material was close to saturation when cored, and some, especially the coarser textured material of the upper profile, was not. This may be due, in part, to the use of air in the drilling process which would tend to dry the material, especially the coarse sections. Though an attempt was made to minimize water loss in the laboratory recoring process, any losses during this process were not quantified. Figure 4 shows a depth profile of field

moisture content and matric potential. In general, the finer textured materials in the lower portion of the profile have greater matric potential for a given moisture content.

This study provides detailed vertical profiling of B-C sedimentary interbed hydraulic properties at one location. As earlier investigations indicate, the sedimentary interbeds are highly complex with variable thickness, texture, and hydraulic properties. The interbed at this location is thicker than average as determined by Anderson and Lewis (1989), and may be in a topographic low in the underlying basalt. It also lacks an impeding clay layer at the top of the

profile as was noted approximately 1.5 km from UZ98-2 by Burgess (1995), though layers of relatively low permeability exist in the bottom 6 m of the profile. As noted in some locations investigated by Hughes (1993), there is a general coarsening of material upward in the profile with fine, possibly low-energy alluvial deposits toward the bottom of the profile.

CONCLUSIONS

The interbed at the location of UZ98-2, approximately 1.2 km southwest of the SDA, is relatively thick and was likely deposited in a fluvial environment. It consists of a 0.3-m thick, highly oxidized gravelly sand layer, a 4.9-m thick sand layer with intermittent gravel, and a 5.5-m thick silt loam layer containing thin, fine sand lenses. Saturated conductivity values range from approximately 3.9×10^{-3} cm/sec for the sand to 2.4×10^{-7} cm/sec for the silt loam. These contrasting layers likely cause perching as water encounters low-permeability layers. The interbed at this location may also contribute to lateral flow through the upper more permeable layers and overlying basalts during seasonal infiltration events such as snowmelt and diversion of water from the Big Lost River to the spreading areas located near UZ98-2.

As has been found in previous interbed investigations, these interbeds are highly variable in character over short distances. The results presented here along with those of past studies, indicate the highly variable nature of the interbeds and the need for further analysis on a large number of samples from various locations and interbeds. Once further measurements are completed and the interbeds are better characterized, correlations between hydraulic properties and particle-size distributions may permit other areas of the INEEL to be more easily assessed.

REFERENCES

Anderson, S.R., and Lewis, B.D., 1989, Stratigraphy of the unsaturated zone at the Radioactive Waste Management Complex, Idaho National Engineering Laboratory, Idaho: U.S. Geological Survey Water-

Resources Investigations Report 89-4065 (DOE/ID-22080), 54 p.

Barracough, J.T., Robertson, J.B., and Janzer, V.J., 1976, Hydrology of the solid waste burial ground, as related to the potential migration of radionuclides, Idaho National Engineering Laboratory: U.S. Geological Survey Open-File Report 76-471 (IDO-22056), 183 p.

Blake, G.R., and Hartge, K.H., 1986, Particle Density. *in* Klute, A. (ed.) *Methods of Soil Analysis, Part 1: American Society of Agronomy, Soil Science Society of America, Madison, Wis., p. 377-382.*

Burgess, D., 1995, Results of the neutron and natural gamma logging, stratigraphy, and perched water data collected during a large-scale infiltration test: EG&G Idaho Inc. Report, ER-WAG7-60, 231 p.

Campbell, G.S., and Gee, G W., 1986, Water Potential: Miscellaneous Methods. *in* Klute, A. (ed.), *Methods of Soil Analysis, Part 1: American Society of Agronomy, Soil Science Society of America, Madison, Wis., p. 628-630.*

Conca, J.L., and Wright, J.V., 1998, The UFA method for rapid, direct measurement of unsaturated transport properties in soil, sediment, and rock: *Australian Journal of Soil Resources*, v. 36, p. 291-315.

Danielson, R.E., and Sutherland P.L., 1986, Porosity. *in* A. Klute, (ed.) *Methods of Soil Analysis, Part 1: American Society of Agronomy, Soil Science Society of America, Madison, Wis., p. 444-445.*

EG&G, 1985, A history of the Radioactive Waste Management Complex at the Idaho National Engineering Laboratory: EG&G Idaho Inc. Report, WM-F1-81-003, 131 p.

Hubbel, J.M., 1990, Perched ground water at the Radioactive Waste Management Complex of the Idaho National Engineering Laboratory: EG&G Idaho Inc. Report, EGG-ER-8779, 73 p.

- Hughes, J.D., 1993, Analysis of characteristics of sedimentary interbeds at the Radioactive Waste Management Complex at the Idaho National Engineering Laboratory, Idaho: Masters Thesis, Idaho State University, 74 p.
- Laney, P.T., Minkin, S.C., Baca, R.G., McElroy, D.L., Hubbell, J.M., Hull, L.C., Russell, B.F., Stormberg, G.J., and Pittman, J.R., 1988, Subsurface investigations program at the Radioactive Waste Management Complex of the Idaho National Engineering Laboratory: U.S. Department of Energy Report, DOE/ID-10183, 354 p.
- Maheras, S.J., Rood, A.S., Magnuson, S.O., Sussman, M.E., and Bhatt, R.N., 1994, Radioactive Waste Management Complex low-level waste radiological performance assessment: EG&G Idaho Inc. Report, EGG-WM-8773, 446 p.
- Mann, L.J., 1986, Hydraulic properties of rock units and chemical quality of water for INEL-1— a 10,365-foot deep test hole drilled at the Idaho National Engineering Laboratory, Idaho: U.S. Geological Survey Water-Resources Investigations Report 86-4020 (IDO-22070), 23 p.
- McElroy, D.L., and Hubbell, J.M., 1990, Hydrologic and physical properties of sediments at the Radioactive Waste Management Complex: EG&G Idaho Inc. Report, EGG-BG-9147, 368 p.
- Mualem, Y., 1976, A new model for predicting the hydraulic conductivity of unsaturated porous media: *Water Resources Research*, v. 12, p. 513-522.
- Nimmo, J.R., and Mello, K.A., 1991, Centrifugal techniques for measuring saturated hydraulic conductivity: *Water Resources Research*, v. 27, p. 1263-1269.
- Nimmo, J.R., Rubin, J., and Hammermeister, D.P., 1987, Unsaturated flow in a centrifugal field: measurement of hydraulic conductivity and testing of Darcy's law: *Water Resources Research*, v. 23, p. 124-134.
- Rightmire, C.T., and Lewis, B.D., 1987, Hydrogeology and geochemistry of the unsaturated zone, Radioactive Waste Management Complex, Idaho National Engineering Laboratory, Idaho: U.S. Geological Survey Water-Resources Investigations Report 87-4198 (DOE/ID-22072), 89 p.
- van Genuchten, M.Th., 1980, A closed-form equation for predicting the hydraulic conductivity of unsaturated soils": *Soil Science Society of America Journal*, v. 44, p. 892-898.
- van Genuchten, M.Th., F.J. Leij, and S.R. Yates, 1991, The RETC Code for Quantifying the Hydraulic Functions of Unsaturated Soils: U.S. Environmental Protection Agency (EPA/600/2-91/065), 85 p.

APPENDIX A

Particle size distribution curves for selected interbed samples from corehole UZ98-2.

